

# Comparison of a Circular Patch Unit Cell Performance for Reflector Applications between Using FR4 and F4BMX220 Substrates at 3.5 GHz Frequency

Taufiqurrachman<sup>a,b,\*</sup>, Mohamad Kamal Abdul Rahim<sup>b</sup>, Dadin Mahmudin<sup>a</sup>, Raden Priyo Hartono Adji<sup>a</sup>, Deni Permana Kurniadi<sup>a</sup>, Winy Desvasari<sup>a</sup>, Sulistyaningsih<sup>a</sup>, Fajri Darwis<sup>a</sup>, Arief Nur Rahman<sup>a</sup>, Prasetyo Putranto<sup>a</sup>, Arie Setiawan<sup>a,c</sup>, Aminuddin Rizal<sup>d</sup>

<sup>a</sup>Research Center for Telecommunication  
National Research and Innovation Agency  
Science and Technology Area Samaun Samadikun, Jl. Sangkuriang  
Bandung, Indonesia

<sup>b</sup>Advanced RF and Microwave Research Group (ARFMRG), Faculty of Electrical Engineering  
Universiti Teknologi Malaysia  
Skudai,  
Johor Baru, Malaysia

<sup>c</sup>Graduate School of Engineering  
Mie University,  
Japan

<sup>d</sup>Electrical Engineering Department  
Politeknik Negeri Semarang  
Jl. Prof. H. Soedarto  
Semarang, Indonesia

## Abstract

This paper presents a performance comparison of the circular patch unit cell as a unit cell for reflector application at 3.5 GHz frequency using a dielectric substrate between FR4 and F4BMX220 substrates. A circular patch is chosen as the unit cell of a reflector because it is commonly used, fabricated, and has a wider bandwidth compared to other structures. A performance comparison of the circular patch on both dielectric substrates is presented in a graph of S-parameters, reflection phase, and operating bandwidth, as well as in the table of dimensions, where the result is performed by simulation using CST software. Based on the simulated results, the F4BMX220 has a better performance compared to the FR4 in terms of the reflection value, operating bandwidth, and dielectric substrate thickness. However, a circular patch diameter when using the F4BMX220 is bigger than when using the FR4 substrate because the FR4 substrate has a higher dielectric constant than the F4BMX220, which is twice the F4BMX220 dielectric constant. Also, the F4BMX220 substrate has a narrower bandwidth compared to the FR4 substrate, which is a difference of around 0.1 GHz. The circular patch when using the F4BMX220 substrate has 0.96 of a reflection value, 0.007 of an absorption value,  $-6.77^\circ$  of the reflection phase, and 0.24 GHz of the operating bandwidth at the normal incident wave angle ( $0^\circ$ ). Also, it can be properly worked if the incident wave angle is moving until  $60^\circ$ . The F4BMX220 substrate has the best performance compared to the FR4 substrate because the reflection value is much better value, even at the incident wave angle of  $60^\circ$ .

**Keywords:** Circular patch, reflector, FR4 substrate, F4BMX220 substrate.

## I. INTRODUCTION

Wireless communication technology is very important in modern communications, along with the development of digital platforms. It is recorded that users increase exponentially every year. Cisco's visual network index states that there will be 28.5 billion network users by the end of 2022 [1]. Based on this, better and more effective technology is a necessity. One of the biggest obstacles in wireless communication systems is the issue

of fluctuations in received signal levels produced by reflection and refraction, which occurs particularly in metropolitan regions with tall buildings and mountainous terrain [2]. In conventional infrastructure, implementing base stations or repeaters [3], as well as reducing cell size [4], is a solution. Still, this technique provides system complexity and can be expensive and difficult to install in certain conditions, particularly in densely populated urban areas. [5]. To effectively overcome these challenges, it is crucial to implement technological advancements.

Recent advancements in the field of metamaterials research have been significant and promising. The term "metamaterials" refers to artificial materials with unique properties not observed in naturally occurring substances [6]–[7]. These artificial materials have the

\* Corresponding Author.

Email:taufiqurrachman@brin.go.id

Received: October 2, 2023 ; Revised: November 27, 2023

Accepted: December 8, 2023 ; Published: December 31, 2023

extraordinary ability to alter the amplitude and phase of electromagnetic waves [6]–[7]. The metamaterial's unit-cell structure can be meticulously arranged to efficiently provide a reflective, transmissive, and absorptive surface. This has several practical uses, including antennas [8], filters [9], lenses [10], absorbers [11], etc. In addition, this artificial material has the potential to solve the problem of decreasing signal levels in wireless communications in urban and hilly environments as an inexpensive, compact, and simple-to-install reflector, as many researchers have demonstrated [12]–[14].

In addition to the cell unit structure of the metamaterial, the selection of material or substrate is frequently a determining factor in the performance of the designed device. The characteristics of the materials employed not only impact the functionality of the device but also contribute to its overall performance. The properties of these materials generate an impact on the response of the metamaterial to electromagnetic waves, including factors such as frequency, reflection, and various other effects. Numerous metamaterial studies have emphasized the substrate as a performance determinant. Several examples of substrates that have been explored include FR4 [15], Rogers RT Duroid 5880 [16], polyimide [17], and ceramic [18]. We can achieve the desired results by selecting the appropriate material and utilizing its properties.

This research focuses on finding the best dielectric substrate between the F4BMX220 and FR4 substrates that is suitable for a circular patch as a reflector application at 3.5 GHz. The FR4 substrate is mostly used in RF and microwave applications because the price is lower than other substrates. The best performance of microwave devices uses the RO5880 Duroid substrate but this substrate has a higher price. The F4BMX220 substrate has similar substrate parameters to the RO5880 Duroid and a low price compared to the RO5880 Duroid, although the F4BMX220 substrate is more expensive than the FR4 substrate. The best dielectric substrate is determined based on the simulated result on CST software, where the simulated result is shown on the graph of the S-

parameters and reflection phase. In addition, the comparison performances of both dielectric substrates are presented by comparing the dimensions of the circular patch and operating bandwidth caused by the incident wave angle effect.

## II. CIRCULAR PATCH DESIGN

A circular patch unit cell for reflector application is designed on two copper layers on a dielectric substrate, where the top layer is a copper circular patch, and the bottom layer is copper of the ground plane. Also, in the middle of two copper layers is a dielectric substrate that is FR4 or F4BMX220. A circular patch dimension can be calculated using (1) to (3) [19]–[20]:

$$r = \frac{F}{\sqrt{\left\{1 + \frac{2h}{\pi \epsilon_r F} \left[ \ln \left( \frac{\pi F}{2h} \right) + 1.7726 \right] \right\}}} \quad (1)$$

$$F = \frac{8.791 \times 10^9}{f_r \sqrt{\epsilon_r}} \quad (2)$$

$$D = 2 \times r \quad (3)$$

where  $r$  is the radius of the circular patch,  $\epsilon_r$  is the dielectric constant of the substrate,  $h$  is the substrate thickness,  $f_r$  is the resonant frequency, and  $D$  is the diameter of the circular patch.

The detailed dimensions of a circular patch unit cell are shown in Figure 1, and Table 1 presents the comparison of dimension between two substrates. The size of both employed substrates are the same; however, the circular patch diameter of the FR4 substrate has a difference of around two times that of the F4BMX220 substrate because the FR4 substrate dielectric constant is 4.3, or around twice the F4BMX220 substrate dielectric constant, which is 2.2. Furthermore, the FR4 substrate is thicker and heavier than the height of the F4BMX220 substrate. The FR4 substrate loss tangent is 0.01 or higher than the F4BMX220 substrate loss tangent, which will affect the reflected power. The smallest loss tangent of the substrate usage will provide the best of the reflected power.

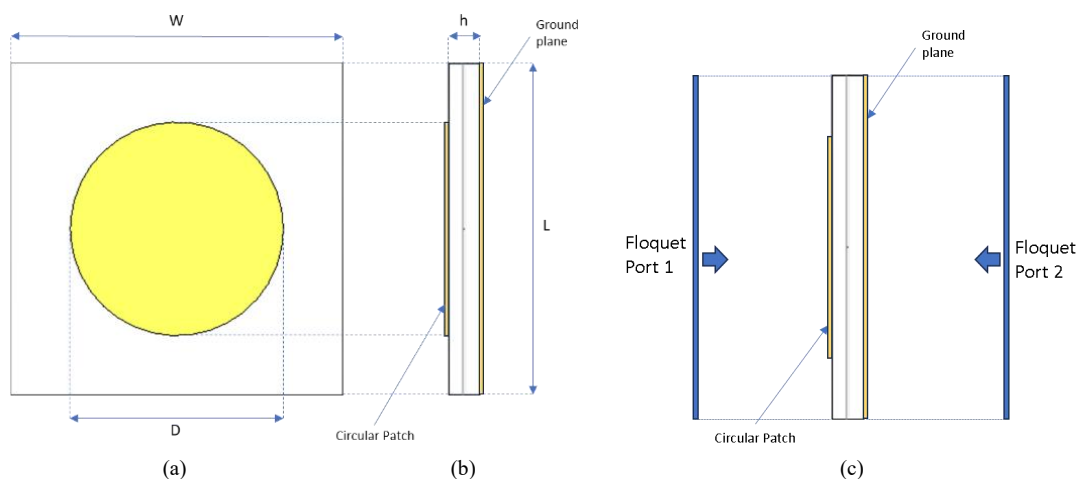


Figure 1. A circular patch unit cell (a) Top view, (b) Side view, (c) The proposed design simulation by using Floquet ports simulation

TABLE 1.  
DIMENSION COMPARISON BETWEEN FR4 AND F4BMX220  
SUBSTRATE.

Type of Substrate	FR4	F4BMX220
Parameters in mm		
Width and Length of substrate, W and L	34.036	
Diameter of circular patch, D	21.82	30.96
Height of substrate, h	3.2	1.5
Copper thickness, t	0.035	
Dielectric constant of substrate, $\epsilon_r$	4.3	2.2
Loss tangent of substrate, $\tan \delta$	0.01	0.001

### III. SIMULATION RESULT AND DISCUSSION

Simulation of the proposed design uses a Floquet port simulation where the horizontal plane is a Perfect Electric Conductor (PEC), and the vertical plane is a Perfect Magnetic Conductor (PMC). The simulation result of the circular patch unit cell between two substrates is shown in Figure 2, where the incident wave angle is through the center of the reflecting element or  $0^\circ$ . Simulation results are presented in a graph of S-parameters and the reflection phase. The S-parameters are shown in  $S_{11}$  as the reflection value and  $S_{21}$  as the absorption value, where  $S_{11}$  and  $S_{21}$  are presented as the magnitude values. The reflection value ( $S_{11}$ ) means how much power is reflected; if  $S_{11}$  has 1, it means the power is fully reflected or deemed a perfect conductor. The absorption value ( $S_{21}$ ) is a value that indicates how much power will be absorbed, which usually depends on the dielectric substrate used in the proposed design.

At 3.5 GHz, using the FR4 substrate yields  $S_{11}$  of 0.62 and  $S_{21}$  of 0.00034. Meanwhile, using F4BMX220 substrate yields  $S_{11}$  of 0.96 and  $S_{21}$  of 0.007. It means that employing the FR4 substrate results in 38.44% reflected power and 0.00001% absorbed power, but employing F4BMX220 substrate results in 92.16%

reflected power and 0.005% absorbed power. As a reflector, using the F4BMX220 substrate has a better advantage in terms of higher reflected power compared to the FR4 substrate. It is caused by the F4BMX220 substrate having a smaller loss tangent ( $\tan \delta$ ) value compared to the FR4 substrate. The way to improve the reflected power of a circular patch unit cell if using the FR4 substrate is to make the substrate thickness thicker, for example, the FR4 substrate thickness is more than 3.2 mm, but it will be bulky. In the reflection phase graph, the proposed design using the FR4 substrate has  $-17.17^\circ$ , but if using the F4BMX220 substrate, it has  $-6.77^\circ$ . It has a different angle of  $10.4^\circ$  but the reflection phase shows a negative angle for both substrates.

Based on Figure 2, the operating bandwidth can be determined by specifying the reflection phase range from  $-90^\circ$  to  $+90^\circ$  where a resonance frequency occurs. The proposed design using the FR4 substrate has an operating bandwidth of around 0.34 GHz, but if using the F4BMX220, it has approximately 0.24 GHz. The operating bandwidth of the FR4 substrate is wider than the operating bandwidth of the F4BMX220 substrate, but the reflected power of the F4BMX220 substrate has better value compared to the FR4 substrate.

Figure 3 shows the E-field and H-field between both substrates at 3.5 GHz which can indicate a power loss in the proposed design. The E-field or H-field intensity of the FR4 has a higher value compared to the F4BMX220. For the E-field in Figures 3.a and 3.b, the power loss distribution concentration is high at the  $+y$  and  $-y$  axes of the proposed design since it is parallel to the electric component of the incident EM wave. For the H-field at Figures 3.c and 3.d, the power loss distribution concentration is high at the  $+x$  and  $-x$  axes of the proposed design since it is parallel to the magnetic component of the incident EM wave.

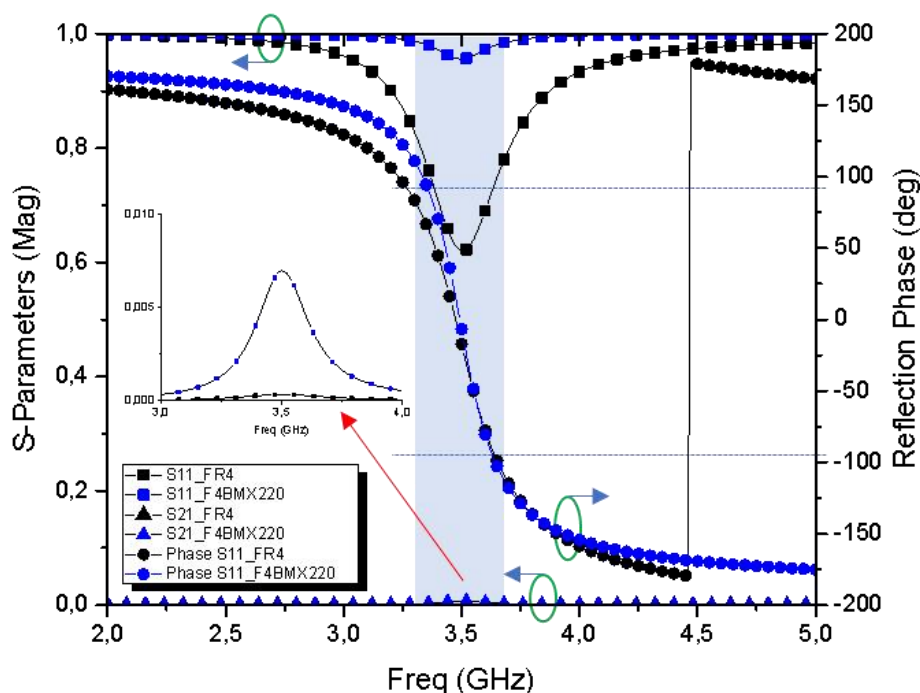


Figure 2. Comparison of S-parameter and reflection phase simulation results for both substrates.

The surface current distribution of both substrates at 3.5 GHz is investigated and shown in Figure 4. The currents flow on the left and right sides of the circular patch, where the currents are going up and down on the

circular patch. A magnetic reaction is also caused by circulating displacement currents between the two metallic elements, which contributes to the proposed structure's losses.

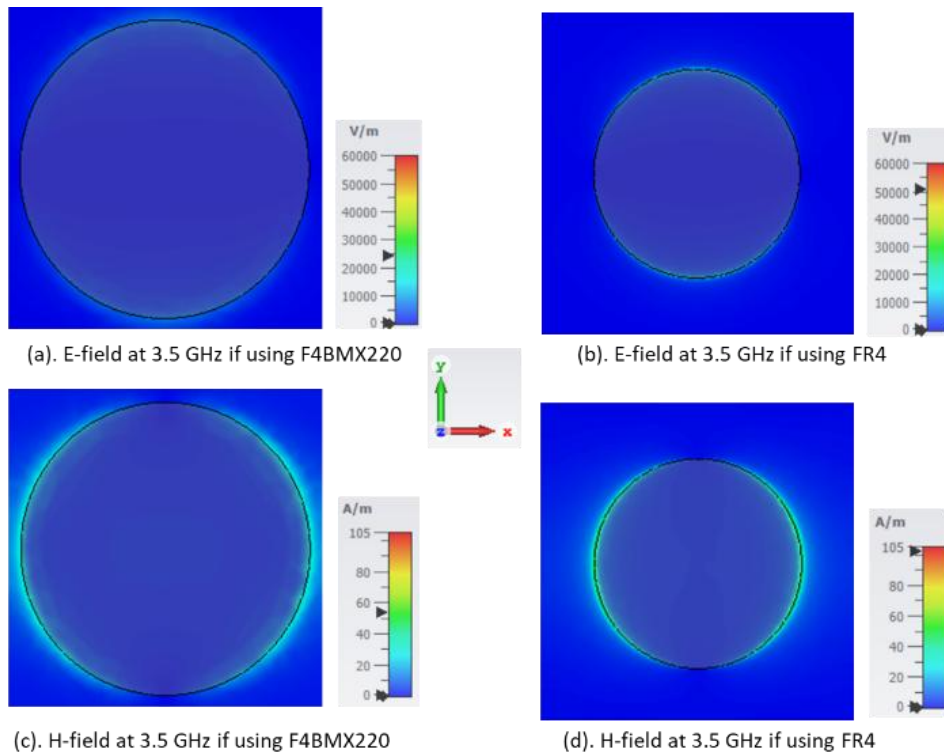


Figure 3. Power loss distribution for the proposed design of both substrates at 3.5 GHz.

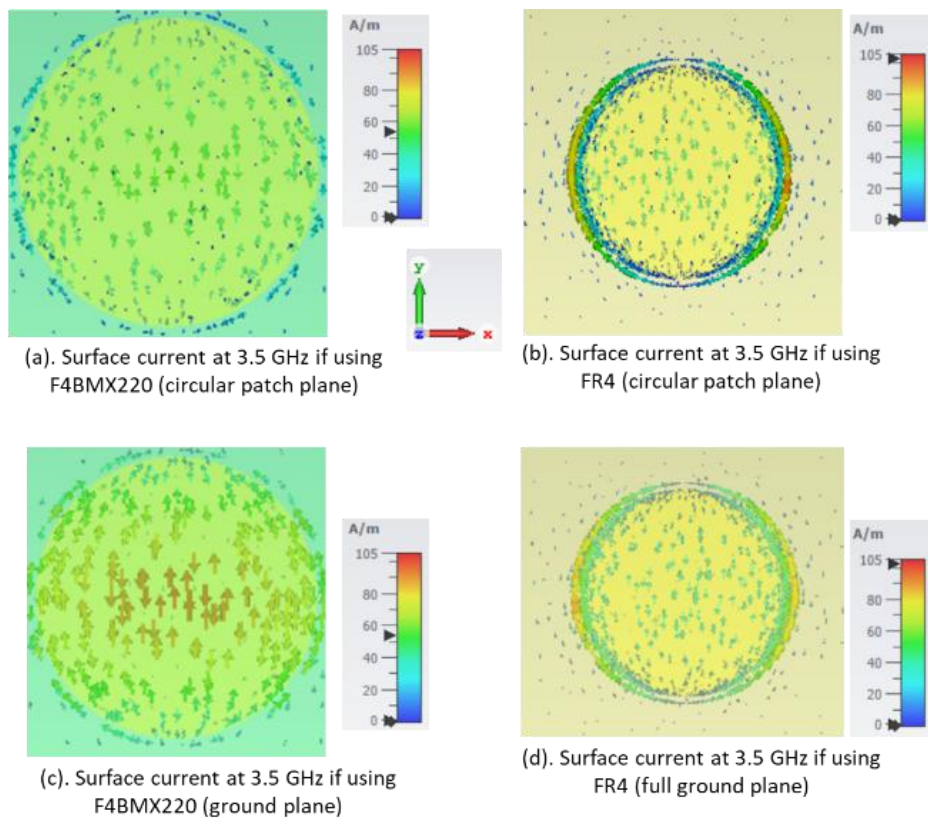


Figure 4. Surface current for the proposed design of both substrates at 3.5 GHz.

In a smart radio environment, a metasurface reflector can be located on the huge buildings' walls or billboards to guide the EM wave to a certain path (users). Usually, the EM wave does not impinge at the center point of the metasurface reflector in real conditions, so the incident wave angle can affect the performance of the metasurface reflector. Figure 5 shows an illustration of the reflection wave angle in the proposed design on two kinds of substrates when the incoming wave angle is moving from 0° to 75°, as notated using  $\theta$ .

**A. F4BMX220 substrate**

The first case, as shown in Figure 6, is the S-parameters and reflection phase graph from the simulation result of the proposed design of the circular patch using a F4BMX220 substrate. When the incident wave angle moves from 0° to 75°, the reflection value ( $S_{11}$ ) decreases from 0.96 at 0° on 3.5 GHz to 0.78 at 75° on 3.54 GHz, and the absorption value ( $S_{21}$ ) increases from 0.007 at 0° on 3.5 GHz to 0.0142 at 75° on 3.54 GHz. According to these simulation results, the reflection value decreases by around 18.75%, and the absorption value increases by around twice. It also has a

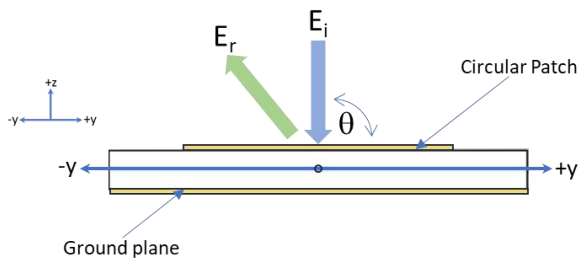


Figure 5. Illustration of the incident wave angle ( $\theta$ ) from 0° to 75° with respect to the reflection phase of the proposed design.

shifting resonance frequency to a higher frequency of around 1.14% at the center frequency in terms of the reflection and absorption values.

Furthermore, the reflection phase shifts from the wide bandwidth to the narrow bandwidth, as shown in Figure 6.b and Table 2. The operating bandwidth will be dropped to 37.5% if the incident wave angle moves from 0° to 60°, but the reflection phase is out of range at the incident wave angle of more than 75°.

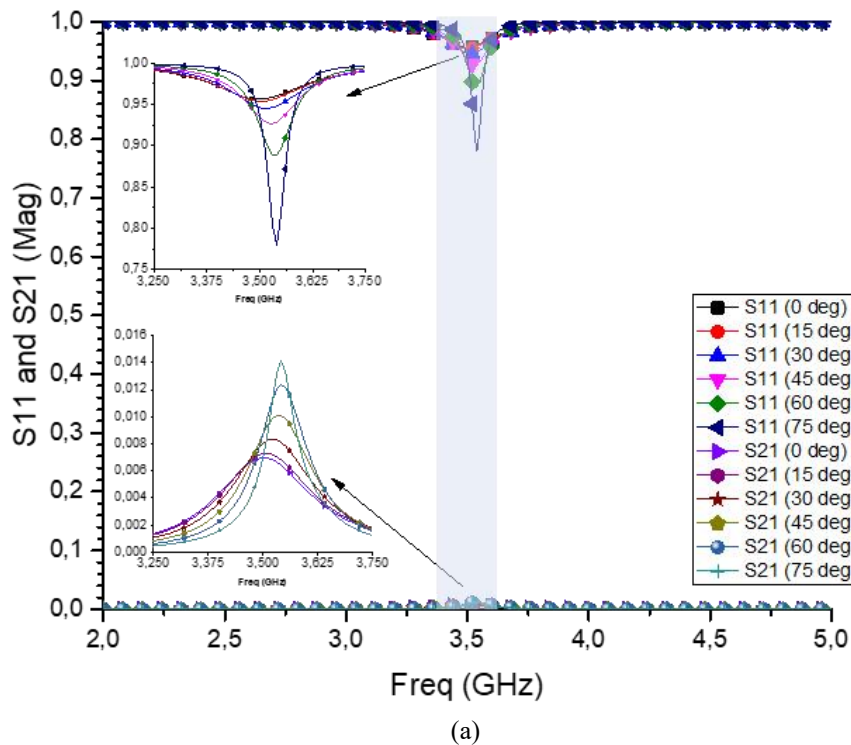
**B. FR4 substrate**

The second case is the proposed design using the FR4 substrate, where the simulated result is shown in Figure 7. The reflection value decreases from 0.69 at 0° on 3.5 GHz to 0.1 at 75° on 3.47 GHz, and the absorption value decreases from 0.001 to 0.172 on 3.5 GHz. It means that the reflection value drops by 85% and shifts to a lower frequency, around 0.03 GHz, but the absorption value increases to 17.1% when the incident wave angle moves from 0° to 75°. In Figure 7.b, the reflection phase will have a narrowed bandwidth because of the incident wave angle effect.

In addition, the operating bandwidth of the effect of the incident wave angle is listed in Table 3. The operating bandwidth is 0.24 GHz at a normal incident wave angle of 0°, but it decreases by around 67.65% if the incident wave moves to 60°. When the incident wave angle is 75° or more, the reflection phase is out of range, so the operating bandwidth cannot be calculated.

TABLE 2. AFFECT THE INCIDENCE WAVE ANGLE TO THE OPERATING BANDWIDTH ON THE F4BMX220 SUBSTRATE

Freq (GHz)	BW (GHz)					
	0	15	30	45	60	75
3,5	0.24	0.23	0.2	0.14	0.09	-



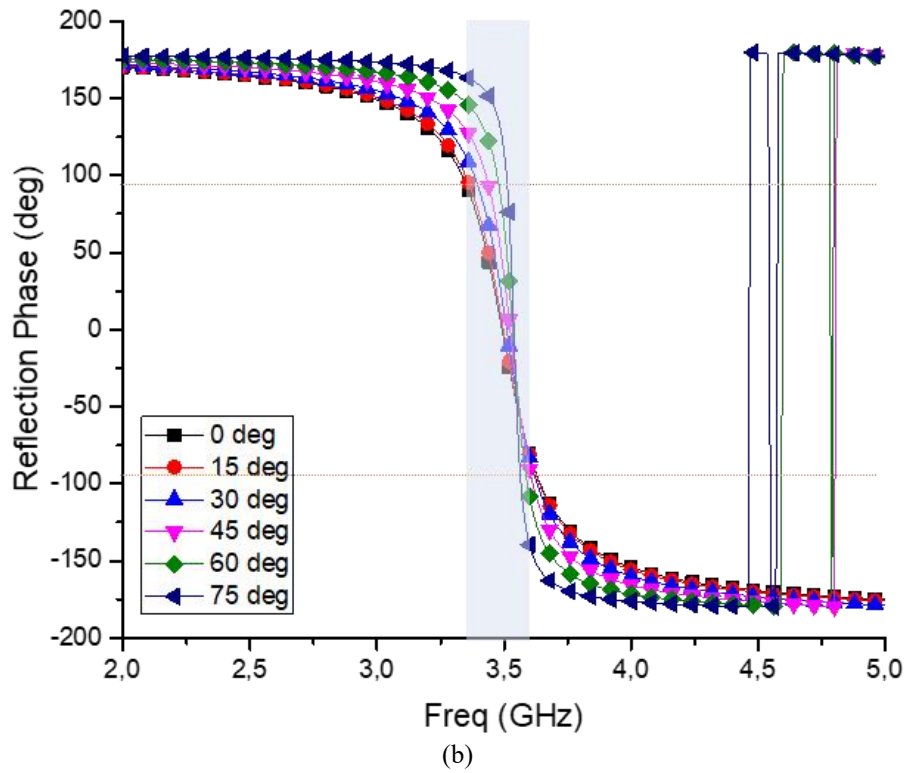
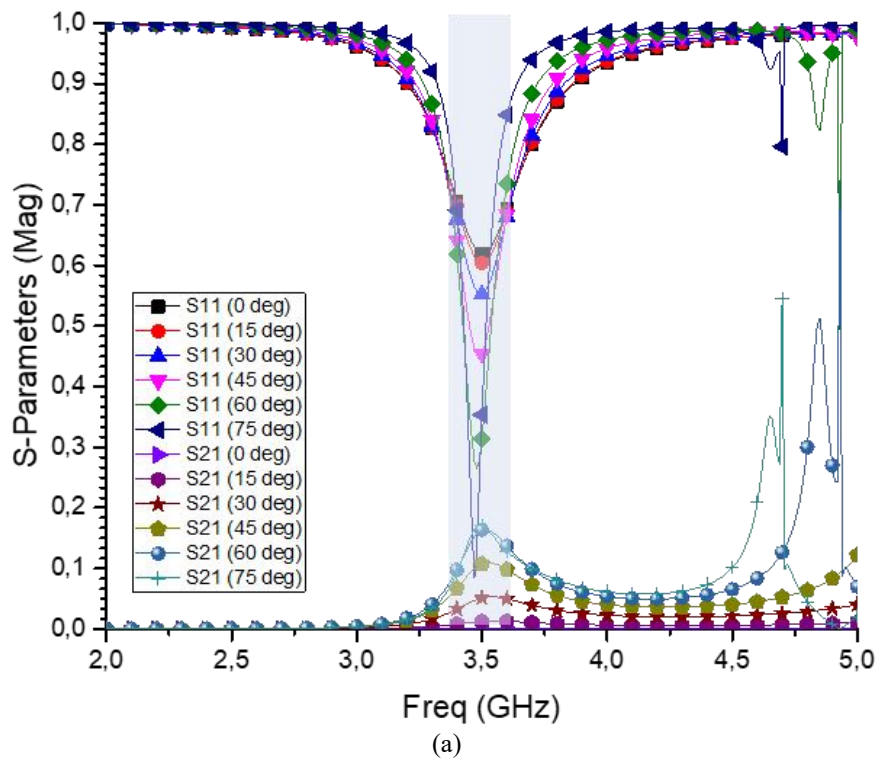


Figure 6. The simulated result when the incident wave angle varies from 0° to 75° on the F4BMX220 substrate: (a). S-Parameters, (b). Reflection Phase.



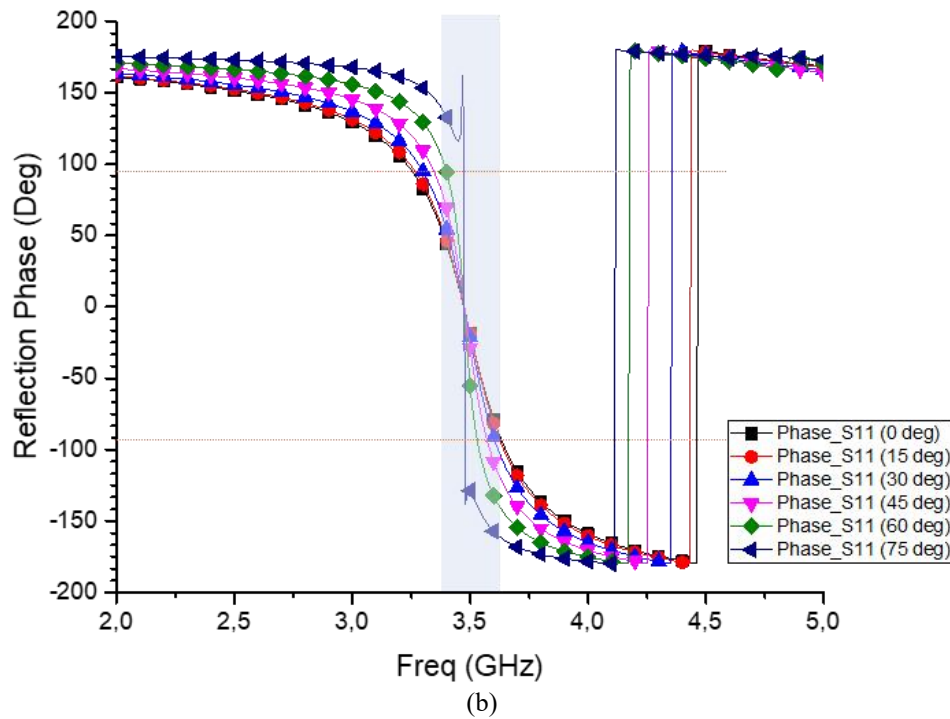


Figure 7. Simulated result if the incident wave angle varies from  $0^\circ$  to  $75^\circ$  on the FR4 substrate: (a). S-Parameters, (b). Reflection Phase.

TABLE 3.  
AFFECT THE INCIDENCE WAVE ANGLE TO THE OPERATING  
BANDWIDTH ON THE FR4 SUBSTRATE

Freq (GHz)	BW (GHz)					
	0	15	30	45	60	75
3.5	0.34	0.32	0.27	0.2	0.11	-

Based on two cases of dielectric substrate usage, the operating bandwidth narrows down when using the F4BMX220 substrate compared to the FR4 substrate, which has a difference of around 0.1 GHz, but the reflection and absorption values are better when using the F4BMX220 substrate than the FR4 substrate.

#### IV. CONCLUSION

The comparison performance of the circular patch designs for reflector applications based on two types of substrates and the effect of the incident wave angle have been presented, designed, simulated, and analyzed. At the normal incident wave angle ( $0^\circ$ ), the proposed design on the F4BMX220 substrate has a reflection value of 0.96, an absorption value of 0.007, and the reflection phase of  $-6.77^\circ$ , but the proposed design on the FR4 substrate has a reflection value of 0.62, an absorption value of 0.00034, and the reflection phase of  $-17.17^\circ$ . It can be caused by the material composition between both substrates, where the F4BMX220 substrate has the smallest  $\tan \delta$  compared to the FR4 substrate. However, the F4BMX220 substrate has a narrower bandwidth than the FR4 substrate, which is a difference of around 0.1 GHz. Based on the simulated results of the incident wave angle effect, the proposed design can work properly if the incident wave angle is from  $0^\circ$  to  $60^\circ$ , but the best performance of the proposed design is when the incident wave angle is at a normal

incident wave angle ( $0^\circ$ ). The F4BMX220 substrate is chosen as a circular patch unit cell for a reflector because it has the best performance in terms of reflection and absorption values, even though the operating bandwidth is narrower than the FR4 substrate.

#### DECLARATIONS

##### Conflict of Interest

The authors have declared that no competing interests exist.

##### CRedit Authorship Contribution

Taufiqurrachman: Conceptualization, Methodology, Software, Validation, Writing-Original Draft; M. Kamal A. Rahim: Conceptualization, Methodology, Supervision, Writing-Reviewing and Editing; Dadin Mahmudin: Validation and Writing-Original Draft; Raden Priyo Hartono Adji: Validation, Investigation, Writing-Original Draft; Dani Permana K: Investigation and Resources; Winy Desvasari: Visualization; Sulistyaningsih: Visualization; Fajri Darwis: Investigation and Resources; Arief Nur Rahman: Visualization and Validation; Prasetyo Putranto: Formal Analysis; Arie Setiawan: Formal Analysis; Aminuddin Rizal: Software and Formal Analysis.

##### Funding

This work was partly supported by Research Organization for Electronics and Informatics (OREI) on Rumah Program Artificial Intelligence, Big Data, dan Teknologi Komputasi (AIBDTK) 2023, under contract number B-298/III.6/PR.03/1/2023.

##### Acknowledgment

This work was partly conducted at the Radio Frequency, Microwave, Acoustic, and Photonics (RFMAP) Lab at the Research Center for Telecommunication, Research Organization for Electronics and Informatics, National Research and Innovation Agency (BRIN), fiscal year of 2023.

## REFERENCES

- [1] "Cisco visual networking index (VNI) global mobile data traffic forecast update, 2017–2022 white paper," Cisco, 2019.
- [2] X. B. Maxama and E. D. Markus, "A survey on propagation challenges in wireless communication networks over irregular terrains," in *Proc. 2018 Open Innov. Conf. (OI)*, Johannesburg, South Africa, 2018, pp. 79–86, doi: 10.1109/OI.2018.8535598.
- [3] D. D. Falconer and J. P. DeCruyenaere, "Coverage enhancement methods for LMDS," *IEEE Commun. Mag.*, vol. 41, no. 7, pp. 86–92, Jul. 2003, doi: 10.1109/MCOM.2003.1215644.
- [4] A. I. Sulyman, A. T. Nassar, M. K. Samimi, et al., "Radio propagation path loss models for 5G cellular networks in the 28 GHz and 38 GHz millimeter-wave bands," *IEEE Commun. Mag.*, vol. 52, no. 9, pp. 78–86, September 2014.
- [5] Z. Peng et al., "An effective coverage scheme with passive-reflector for urban millimeter-wave communication," *IEEE Antennas Wirel. Propag. Lett.*, vol. 15, pp. 398–401, 2016, doi: 10.1109/lawp.2015.2447734.
- [6] V. G. Veselago, "The electrodynamics of substances with simultaneously negative values of  $\epsilon$  and  $\mu$ ," *Soviet Phys. Uspekhi*, vol. 10, no. 4, pp. 509–514, Apr. 1968, doi: 10.1070/pu1968v010n04abeh003699.
- [7] D. R. Smith, W. J. Padilla, D. C. Vier, S. C. Nemat-Nasser, and S. Schultz, "Composite medium with simultaneously negative permeability and permittivity," *Phys. Rev. Lett.*, vol. 84, no. 18, pp. 4184–4187, May 2000, doi: 10.1103/physrevlett.84.4184.
- [8] B. Niu and J. Tan, "Compact four-element MIMO antenna using T-shaped and anti-symmetric U-shaped slotted SIW cavities," *Electron. Lett.*, vol. 55, no. 19, pp. 1031–1032, Sep. 2019, doi: 10.1049/el.2019.2142.
- [9] A. A. Fathnan, . Taufiqqurqchman., Y. N. Wijayanto, D. Mahmudin, and P. Daud, "Efek kopling pada filter metamaterial coplanar waveguide menggunakan SRRS persegi panjang horizontal," *J. Elektr. Telekom.*, in Indonesian, vol. 15, no. 1, pp. 18–22, Jun. 2016, doi: 10.14203/jet.v15.18-22.
- [10] J. Yang, C. Huang, J. Song, X. Zhang, X. Xie, and X. Luo, "Metasurface-based lens for antenna gain enhancement and radar cross section reduction," *IEEE Photon. J.*, vol. 11, no. 6, pp. 1–9, Dec. 2019, doi: 10.1109/jphot.2019.2950194.
- [11] S. A. Mohammed, R. A. Kamil Albadri, and K. S. L. Al-Badri, "Simulation of the microwave five-band a perfect metamaterial absorber for the 5G communication," *Heliyon*, vol. 9, no. 9, Sep. 2023, Art. No. e19466, doi: 10.1016/j.heliyon.2023.e19466.
- [12] B. C. Nguyen, T. Q. Pham, N. N. Thang, T. M. Hoang, and P. T. Tran, "Improving the performance of wireless half-duplex and full-duplex relaying networks with intelligent reflecting surface," *J. Franklin Institute*, vol. 360, no. 4, pp. 3095–3118, Mar. 2023, doi: 10.1016/j.jfranklin.2023.01.030.
- [13] M. D. Gregory et al., "A low cost and highly efficient metamaterial reflector antenna," *IEEE Trans. Antennas Propag.*, vol. 66, no. 3, pp. 1545–1548, Mar. 2018, doi: 10.1109/tap.2017.2781151.
- [14] A. Hoque, M. T. Islam, A. F. Almutairi, and M. E. H. Chowdhury, "DNG metamaterial reflector using SOCT shaped resonator for microwave applications," *IEEE Access*, vol. 9, pp. 59148–59159, 2021, doi: 10.1109/access.2021.3071472.
- [15] Z. He, J. Jin, Y. Zhang, and Y. Duan, "Design of a two-dimensional "T" shaped metamaterial with wideband, low loss," *IEEE Trans. Appl. Supercond.*, vol. 29, no. 2, Mar. 2019, Art no. 1100204, doi: 10.1109/TASC.2018.2889356.
- [16] S. Tariq, S. I. Naqvi, N. Hussain, and Y. Amin, "A metasurface-based MIMO antenna for 5G millimeter-wave applications," *IEEE Access*, vol. 9, pp. 51805–51817, 2021, doi: 10.1109/ACCESS.2021.3069185.
- [17] S. M. R. H. Shawon, S. Kapali, I. B. F. Rahman, S. Islam, and K. Ali, "Switchable THz guided mode enhancement in subwavelength thick PTFE — polyimide based metamaterial devices," *IEEE Access*, vol. 11, pp. 77919–77928, 2023, doi: 10.1109/ACCESS.2023.3298298.
- [18] Z. Liu, P. Wang, and Z. Zeng, "Enhancement of the gain for microstrip antennas using negative permeability metamaterial on low temperature co-fired ceramic (LTCC) substrate," *IEEE Antennas Wirel. Propag. Lett.*, vol. 12, pp. 429–432, 2013, doi: 10.1109/LAWP.2013.2254697.
- [19] Ouboudrar Ismail, Lagmich Youssef, Oulhaj Otman and Amina Aghanim, "Design of a circular patch antenna with a reflector for GPR applications," in *Proc. ITM Web Conf.*, vol. 48, 2022, Art. no. 01004, doi: 10.1051/itmconf/20224801004R.
- [20] C. Saetiaw, C. Taonok, and S. Summart, "Design of modified-circular patch antenna with AMC reflector for WLAN applications," in *Proc. 2018 15th Inte. Conf. Electric. Eng. Electron. Comp. Telecomm. Inf. Tech. (ECTI-CON)*, Chiang Rai, Thailand, 2018, pp. 213–216, doi: 10.1109/ECTICon.2018.8619886.